JCTC Journal of Chemical Theory and Computation

# Multiple Low-Lying States for Compound I of $P450_{cam}$ and Chloroperoxidase Revealed from Multireference Ab Initio QM/MM Calculations

Hui Chen,*,† Jinshuai Song,†,‡ Wenzhen Lai,† Wei Wu,‡ and Sason Shaik*,†

*Institute of Chemistry and the Lise Meitner-Minerva Center for Computational Quantum Chemistry, Hebrew University of Jerusalem, Givat Ram Campus, 91904 Jerusalem, Israel, State Key Laboratory of Physical Chemistry and Chemical Engineering, Xiamen University, 361005 Xiamen, P. R. China*

Received November 23, 2009

**Abstract:** The hybrid CASPT2/MM approach is employed to systematically study the ground and low-lying excited states of the ultimate active species of the enzymes $P450_{cam}$ and chloroperoxidase (CPO): the oxoiron(IV)−porphyrin cation−radical $Por^{\bullet+}Fe^{IV}$═O(Cys) species, the so-called Compound I (Cpd I). The results underscore the fact that the B3LYP/MM method is quite accurate on the most part. However, the CASPT2/MM energies for the ferryl-pentaradicaloid quartet state and the perferryl $Fe^{V}O$ doublet and quartet states are significantly lower than the B3LYP/MM results. Thus, while the present CASPT2/MM may still overestimate the stability of these states, nevertheless, taken at its face value, the result raises the question whether these states actually contribute to the reactivity of Cpd I. Our paper tries to grapple with this question in view of (a) the recent speculations that the perferryl $Fe^{V}O$ states may be involved in unusual reactivities of Cpd I species (Pan, Z. Z.; Wang, Q.; Sheng, X.; Horner, J. H.; Newcomb, M. *J. Am. Chem. Soc.* **2009**, *131*, 2621−2628) and (b) the DFT/MM results which show that the pentaradicaloid states have intrinsically low barriers for H-abstraction (Altun, A.; Shaik, S.; Thiel, W. *J. Am. Chem. Soc.* **2007**, *129*, 8978−8987). The application of CASPT2/MM to high valent transition metal states like the perferryl are far from being trivial, and the experience and insight gained in this study are expected to be helpful for future successful application of this type of method to resolve key issues in P450 reactivity.

## Introduction

It is generally accepted that the reactive species in the thiolate-ligated heme enzyme cytochromes P450 (P450s)[1,2a] and chloroperoxidase[2] (CPO) is the oxoiron(IV) porphyrin $\pi$-cation radical active species $Por^{\bullet+}Fe^{IV}$═O(Cys), termed Compound I (Cpd I), which is responsible for the potent catalytic monooxygenase and peroxidase activities of these enzymes and has the electronic structure shown in Scheme 1. While Cpd I in CPO has been characterized by many spectroscopic methods,[3] the corresponding species in P450s is still elusive in the native catalytic cycle.[1,4] To bypass these difficulties, P450 Cpd I species were generated directly, by reacting the enzyme with *m*-chloroperoxybenzoic acid, and were followed using rapid scan stopped-flow absorption spectroscopy.[5] Very recently, P450 Cpd I species were produced also by laser flash photolysis (LFP) of the one-electron reduced species, in a manner that enabled the following of their reactivity patterns toward a variety of substrates.[6] These studies questioned the consensus that the reactive state for P450 in the native cycle is the $\pi$-cation radical ferryl state, $Por^{\bullet+}Fe^{IV}$═O(Cys).

Thus, the elusive nature of Cpd I in the native P450 cycle has generated alternative hypotheses regarding the nature of the "active oxidant" of P450. One of the species that has

* Corresponding author fax: +972 (0)2 658 4033; e-mail: chenh@yfaat.ch.huji.ac.il (H.C.), sason@yfaat.ch.huji.ac.il (S.S.).
† Hebrew University of Jerusalem.
‡ Xiamen University.

10.1021/ct9006234 
Published on Web 02/19/2010

***Scheme 1.*** Orbital Diagram for the Doublet Ground State of Cpd I Species in $P450_{cam}$ and CPO on the Basis of DFT/MM Calculation

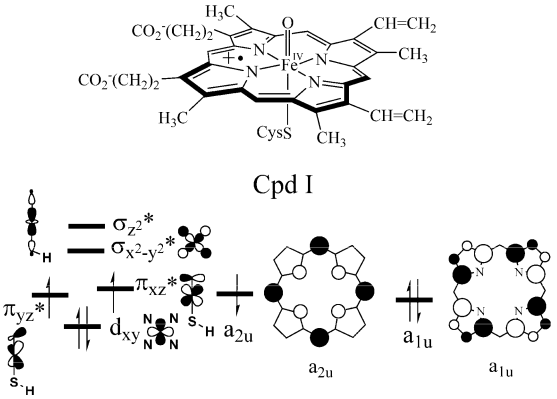


recently been invoked to explain the high reactivity of $P450_{cam}$ compared with those of the LFP-generated Cpd I species is the perferryl, $PorFe^{V}=O$,[6] in which the porphyrin gets one electron from one of the orbitals ($d_{xy}$ or $\pi^*$) in the d-block of iron to become closed-shell (see Scheme 1). Another state that has been revealed by density functional theory (DFT)[7] and DFT/MM calculations[8,9] is the pentaradicaloid state, in which an electron from the $d_{xy}$ (also called $\delta$) orbital of the triradicaloid state, in Scheme 1, is promoted to the $\sigma^*_{x^2-y^2}$ orbital. This latter state has just recently been speculated as a possible cause of the extremely high reactivity of a model Cpd I species.[10]

Due to the prominent role played by Cpd I in P450s chemistry and its elusive status, within the native catalytic cycle, it has been extensively studied by the hybrid quantum mechanical/molecular mechanical (QM/MM) approach,[11] which accounts for effects associated with the protein environment. The major QM tool has so far been DFT/MM, which basically gave results compatible with DFT-only calculations that included bulk polarity and hydrogen bonding (H-bonding) effects due to NH···S interactions with the thiolate ligand. However, it has been obvious that further studies should ultimately be carried out at the ab initio level with the multireference configuration interaction (MRCI) or multireference second-order perturbation (MRPT2) with an adequate basis set and a large active space. In this work, we report such a study of this key species, for the two heme enzymes, based on high level ab initio multiconfigurational second-order perturbation[12] CASPT2/MM calculations, with an aim of establishing the state ordering of all the low-lying states within around 30 kcal/mol, the lower ones of which could possibly contribute to the reactivity of this species.

Three ab initio multireference studies have been reported so far, which addressed either the gas phase species or were limited to a few states.[8,13,14] Thus, Thiel and co-workers used the difference dedicated configuration interaction (DDCI2) method[8] and, later, DDCI2-Q with MR-Davidson correction (which treats the size-consistency problem of CI) to conduct QM/MM calculation on Cpd I of $P450_{cam}$.[13] The quartet $a_{2u}$ triradicaloid state, having the electronic structure in Scheme 1 ($a_{2u}^1\pi^*_{yz}{}^1\pi^*_{xz}{}^1$), but with all electrons being spin-up, was found to be the lowest quartet state in DFT/MM calculations[8,9] but only slightly lower (1.9 kcal/mol) than the corresponding $a_{1u}$ triradicaloid state ($a_{1u}^1\pi^*_{yz}{}^1\pi^*_{xz}{}^1$) at the DDCI2-Q/MM level.[13] However, the corresponding calculation for the doublet state with the large active space encountered convergence problems. So with large active space, no states other than the quartet triradicaloid $a_{1u}$ and $a_{2u}$ states were explored to date using in-protein calculations. Radoń et al.[14] used the CASPT2 method to study a Cpd I model of P450 in the gas phase and found that multistate CASPT2 was crucial for generating the porphyrin-based cation radical state as the ground state. Inclusion of the axial thiolate ligand orbital into the active space seemed to be necessary because the sulfur-based radical state was significantly lower in energy than the porphyrin-based triradicaloid state at the complete active space self-consistent field (CASSCF) level that precedes the CASPT2 calculations. So the situations in gas phase and in protein calculations of Cpd I appear very different. This difference was also exhibited by gas phase DFT studies[15] which revealed a ground state with a high sulfur radical character, vis-à-vis in protein DFT/MM calculations,[8,11] which showed a dominant porphyrin-based radical structure. By contrast to the gas phase results, in CPO, where Cpd I is observable, electron−nuclear double resonance (ENDOR) measurements have shown that the thiolate spin density of Cpd I is less than 0.23,[3e] which supports the DFT/MM[8,11] and the DDCI2/MM results.[13] It is apparent therefore that QM/MM treatments based on ab initio multireference correlated methods for the important open-shell Cpd I system are essential but have still not been used to describe a variety of low lying states that might be contributing to the reactivity of this species. There are many important and interesting questions to be answered in this field. As we mentioned above, DFT[16] and DFT/MM[9] calculations have shown that the pentaradicaloid states of Cpd I in P450 could be more reactive than the triradicaloid ground state. But how high is the pentaradicaloid state in energy relative to the triradicaloid ground state for Cpd I species? B3LYP[7,16] and B3LYP/MM calculations[8,9] for $P450_{cam}$ suggested that this state is adiabatically about 14 and 12 kcal/mol higher than the ground state, respectively. However, previous spectroscopy-oriented configuration interaction (SORCI) calculations on model nonheme iron-oxo systems[8,17] suggested that the state having an iron $d_{xy}{}^1\sigma^*_{x^2-y^2}{}^1$ configuration (two iron d-type orbitals spanning the equatorial plane), analogous to the pentaradicaloid state in Cpd I, and the state having a $d_{xy}{}^2\sigma^*_{x^2-y^2}{}^0$ configuration, analogous to the triradicaloid state in Cpd I, are close in energy. Another intriguing question is how high the perferryl $Fe^{V}$-oxo species are in Cpd I, which has been repeatedly proposed to be the actual reactive species in native P450 chemistry.[6,18] According to recent TD-DFT/MM calculations of $P450_{cam}$ Cpd I, these $Fe^{V}$ states are at least 37 kcal/mol higher in energy relative to the doublet ground state triradicaloid state (Scheme 1) and hence cannot possibly contribute to reactivity.[9] In order to answer these questions using a high-level wave function theory, we decided to carry out systematic CASPT2/MM calculations of both the ground state of Cpd I and its low lying excited states. Thus, while the present results may certainly not be the last word on Cpd I, still they constitute state-of-the-art values that will provide a challenge to proceed to even higher

QM/MM levels, with an aim of establishing a broader and deeper understanding of the electronic structures of Cpd I of thiolate enzymes and its potential as a multistate reactivity (MSR) reagent.

**The Computational Methodology.** *DFT/MM Calculations.* The QM/MM setup procedure used here for $P450_{cam}$ and CPO was described extensively in our previous works.[19] Here, we addressed only the essential features and relegated the rest of the details to the Supporting Information (SI) document.

All DFT/MM computations were performed using ChemShell[20] interfaced with Turbomole[21] and DL_POLY.[22] The hybrid B3LYP[23] functional was used for the QM region, and the CHARMM22[24] force field was used for the MM region. The geometries were optimized with the double-ζ LACVP[25] basis set (B1), followed by a single-point energy correction with a larger basis set B2, and the Wachters' all electron basis set[26] augmented with diffuse d and polarization f functions on iron (8s7p4d1f) and 6-31++G(d,p)[27] on the other atoms. The QM region in our QM/MM calculations involves porphine with an iron-oxo unit and axial cysteine ligand modeled as SH. The electronic embedding scheme[28] was used to account for the polarization effect of the QM part induced by the protein environment. No cutoffs were introduced for the nonbonding MM and QM/MM interactions. The dangling bond at the QM/MM boundary was saturated by a hydrogen-link atom and treated in the framework of the charge-shift method.[28] Full geometry optimizations were performed with HDLC optimizer.[29] No symmetry constraints were imposed on the studied Cpd I systems.

*CASPT2/CASSCF/MM Calculations.* The multireference ab initio CASPT2/CASSCF/MM calculations were carried out with the MOLCAS 7.2 suite of programs[30] using geometries optimized at the B3LYP/MM level. The QM-polarizing point charges generated in the DFT/MM geometry optimization were used during the CASPT2/CASSCF/MM procedure. The Douglas−Kroll−Hess Hamiltonian[31] was used to account for the scalar relativistic effects. A large basis set was required in the CASPT2/CASSCF calculations: On iron, we used a triple-ζ cc-pwCVTZ-DK basis set (Fe, 9s8p6d3f2g),[32] which can handle the 3s3p semicore correlation of Fe well. For the six atoms of the immediate coordination sphere, we employed a triple-ζ cc-pvTZ-DK basis set (O, N, 4s3p2d1f; S, 5s4p2d1f),[33] while for the rest of the system we used the double-ζ cc-pvDZ-DK basis set (C, 3s2p1d; H, 2s1p).[33] The total number of basis functions is 631.

Cholesky decomposition (CD) techniques[34] were used during the CASPT2/CASSCF calculations with a well-tested threshold of $10^{-4}$ (see Table S1 in the SI) to reduce the computational time and disk storage requirements. All valence electrons plus the 3s and 3p electrons of iron were correlated in the CASPT2 calculations. To bracket more critically the results, the CASPT2 calculations used two types of zero order Hamiltonians: the standard IPEA zero-order Hamiltonian, using an orbital energy shift correction by the gap between ionization potential (IP) and electron affinity (EA) of active orbitals, i.e., IPEA shift = 0.25. This latter procedure is suggested in MOLCAS, as a method of choice, for reducing systematic errors of calculated gaps between states having different numbers of unpaired electrons.[35] However, to the best of our knowledge, there are still no systematic calibrations to show that this IPEA shift value provides better results for other cases, i.e., in isogyric processes where the number of unpaired electrons is kept constant. Therefore, we used also a second zero-order Hamiltonian (IPEA shift = 0), which is the original formulation, and applied it for some triradicaloid states with three unpaired electrons such as the $a_{1u}$ singly occupied states, quartet $Fe^V$ states, and sulfur-based triradicaloid states. An imaginary level shift of 0.1 au was used in the CASPT2 calculation to avoid the intruder state problem.[36]

As already noticed by Radoń et al. in their gas phase calculation,[14] state-average CASSCF orbitals could be far from optimal for any of the states involved. So in this work, wherever possible, we used state-specific calculations to compute one state at a time. For higher excited states for which state-specific calculations were not possible due to root flipping, we performed state-average calculations followed by multistate (MS) CASPT2 calculations[37] to improve the possible deficiency of the state-average reference CASSCF wave function.

The used QM region and active orbitals are shown in Figure 1. The 14 orbitals depicted in the figure formed an active space of 15 electrons distributed in 14 orbitals, labeled as (15,14). The active space includes for the first time all iron 3d orbitals, and this enables us to explore all the possible configurations within the iron valence 3d shell. The $4d_{xy}$ orbital and $4d_{yz}+3p_y$ and $4d_{xz}+3p_x$ are orbitals accounting for the so-called "double-shell" effect[12] in Cpd I and are found to be important for a balanced treatment of states wherein an electron is excited out of the $3d_{xy}$ (as in the case of the pentaradicaloid state) or Fe−O $\pi$ type orbitals (as in the case of doublet $Fe^V$ states). The latter two orbitals were first included in the active space by Neese and Thiel et al. in their DDCI2-Q/MM calculation for Cpd I in $P450_{cam}$.[13] These two orbitals are seen in Figure 1 to be combinations of iron 4d and oxygen 3p orbitals rather than pure iron 4d orbitals because of strong covalent interaction between Fe and O of the iron-oxo moiety. All three of the above empty orbitals for the "double-shell" effect were also found to have an additional beneficial effect of stabilizing the active space used here.

Using CASSCF(15,14) calculations (see Table S2−S3 in SI), we found that the states characterized by singly occupied porphyrin $a_{1u}$ or $a_{2u}$ orbitals can be studied separately with active spaces that exclude the corresponding $a_{2u}$ or $a_{1u}$ orbitals. This finding enabled us to use two (13,13) active spaces generated from (15,14) by moving the $a_{1u}$ or $a_{2u}$ orbital out of active space and thereby studying more economically the $a_{2u}$ or $a_{1u}$ singly occupied states. For sulfur-based radicaloid states, it was necessary to introduce two sulfur-based $\sigma_S$ and $\pi_S$ orbitals, which are the sulfur lone pair orbitals, the former one pointing toward iron and the latter being perpendicular to the Fe−S−H plane. These two orbitals are not shown in Figure 1 since they are only used to calculate the sulfur-based radicaloid states. The active

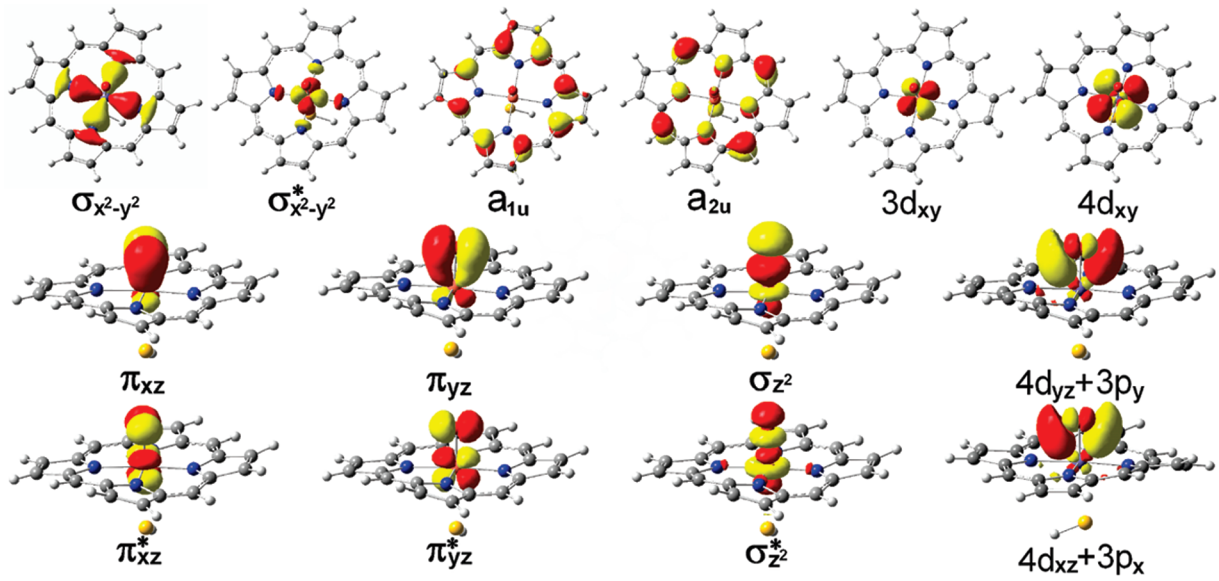


***Figure 1.*** Active orbitals used to generate active space (15,14). The contour value is ±0.05 e/au$^3$.

space employed for the sulfur-based radicaloid states $\Pi_S/\Sigma_S$ was generated from the one shown in Figure 1, by replacing the $a_{1u}$ and $a_{2u}$ orbitals with sulfur-based $\pi_S/\sigma_S$ orbitals.

For simplicity, the various states are conventionally labeled by the orbital that accommodates the free radical; we use superscripts to represent spin multiplicity of the state, and in parentheses we add the formal oxidation state of iron; e.g., $^2A_{2u}(Fe^{IV})$ represents the triradicaloid $Fe^{IV}$ state in Scheme 1, while $^4\Delta_{xy}(Fe^{V})$ represents the quartet $Fe^{V}$ state in which iron $3d_{xy}$ ($\delta$) orbital is singly occupied. If there is more than one state for a given label, we add a serial number before the label to indicate energy ordering at the CASPT2/MM level, e.g., 2 $^2A_{2u}(Fe^{IV})$ represents the second $Fe^{IV}$ doublet state, in which porphyrin $a_{2u}$ orbital is mainly singly occupied. The singly occupied orbitals are specified in the fifth columns of Tables 2 and 5. Schemes 2 and 3 further show the simple orbital diagram for these states.

## Results and Discussion

As was shown in the previous theoretical work on model nonheme iron-oxo species,[17a] some geometric parameters such as equatorial Fe−N bond distances are quite important for the energy gap of different states. Therefore, we first summarize the key bond distances of Cpd I obtained from B3LYP/MM calculations for CPO and $P450_{cam}$ in Table 1. It can be seen that, for CPO, where experimental data of extended X-ray absorption fine structure (EXAFS) measurement are available,[38] the bond distances all agree well with the experimental results, except for the Fe−S bond distance, which is about 0.1 Å longer in the calculated geometry. From previous calculations for iron-oxo species as well as our own test calculation at the DFT/MM level (see Table S4 in SI), this geometric difference is not likely to affect the energetic levels of the states we are interested in.

Our main results at the CASPT2/CASSCF/MM level are summarized in Tables 2−5 for Cpd I of CPO and $P450_{cam}$. We calculated 11 doublet and 9 quartet states for each enzyme in Tables 2 and 5. Unless specified, all the relative energy data that we used from ab initio multireference calculations refer to the ones at the CASPT2/MM level. Identification of the various states can be aided by the orbital occupancies in the tables and in Schemes 2 and 3. The full set of results is summarized in the Supporting Information document, while below we present only the key results.

**A. Triradicaloid $Fe^{IV}$ Doublet and Quartet States.** As seen from Table 2 and Scheme 2, for CPO and $P450_{cam}$, our lowest doublet and quartet triradicaloid states (**1** and **10**) at the CASPT2/MM level correspond, with one exception, to the lowest two states in DFT/MM calculations, in which porphyrin $a_{2u}$ and two Fe−O $\pi^*$ orbitals are singly occupied, with good accord between the two sets of results. Thus, in agreement with B3LYP/MM, the quartet state, 1 $^4A_{2u}(Fe^{IV})$, is very slightly higher (by 0.6 to 0.9 kcal/mol) in energy than the corresponding doublet state, 1 $^2A_{2u}(Fe^{IV})$, which is stabilized slightly by the antiferromagnetic coupling $S = 1$ iron-oxo ferryl unit and $S = 1/2$ porphyrin radical in the thiolate-ligated Cpd I system. This suggests that DFT and DFT/MM are quite reliable in describing the quartet and doublet ground states of Cpd I. The second triradicaloid doublet state 2 $^2A_{2u}(Fe^{IV})$ (**5**), which involves singlet pairing of the electrons in the two $\pi^*$ orbitals, and a singly occupied $a_{2u}$, was located to lie about 18 kcal/mol higher above the ground state **1**, which is comparable with gas phase B3LYP calculations reported before for Cpd I[39] and nonheme iron-oxo species.[40] As such, these states for either CPO or P450cam are not likely to be accessible for reactivity, since most calculated barriers for hydroxylation and epoxidation are lower than this value.[41] We also calculated two other triradicaloid quartet states 3 $^4A_{2u}(Fe^{IV})$ and 4 $^4A_{2u}(Fe^{IV})$ (**15** and **16**) where one of the two electrons in two $\pi^*$ orbitals is excited to the Fe−N antibonding $\sigma^*_{x^2-y^2}$ orbital. Their high relative energy (more than 26 kcal/mol) indicates they are even less likely than state **5** to affect the reactivity of Cpd I.

**B. The Pentaradicaloid $Fe^{IV}$ Quartet State.** From Table 2, the pentaradicaloid $Fe^{IV}$ quartet state 2 $^4A_{2u}(Fe^{IV})$ (**11**), having five unpaired electrons, is very close (within 2 kcal/

***Scheme 2.*** Schematic Representation of Orbital Occupancies of the Main Electronic Configurations of Various (a) Doublet and (b) Quartet States of Cpd I Calculated in Table 2[a]

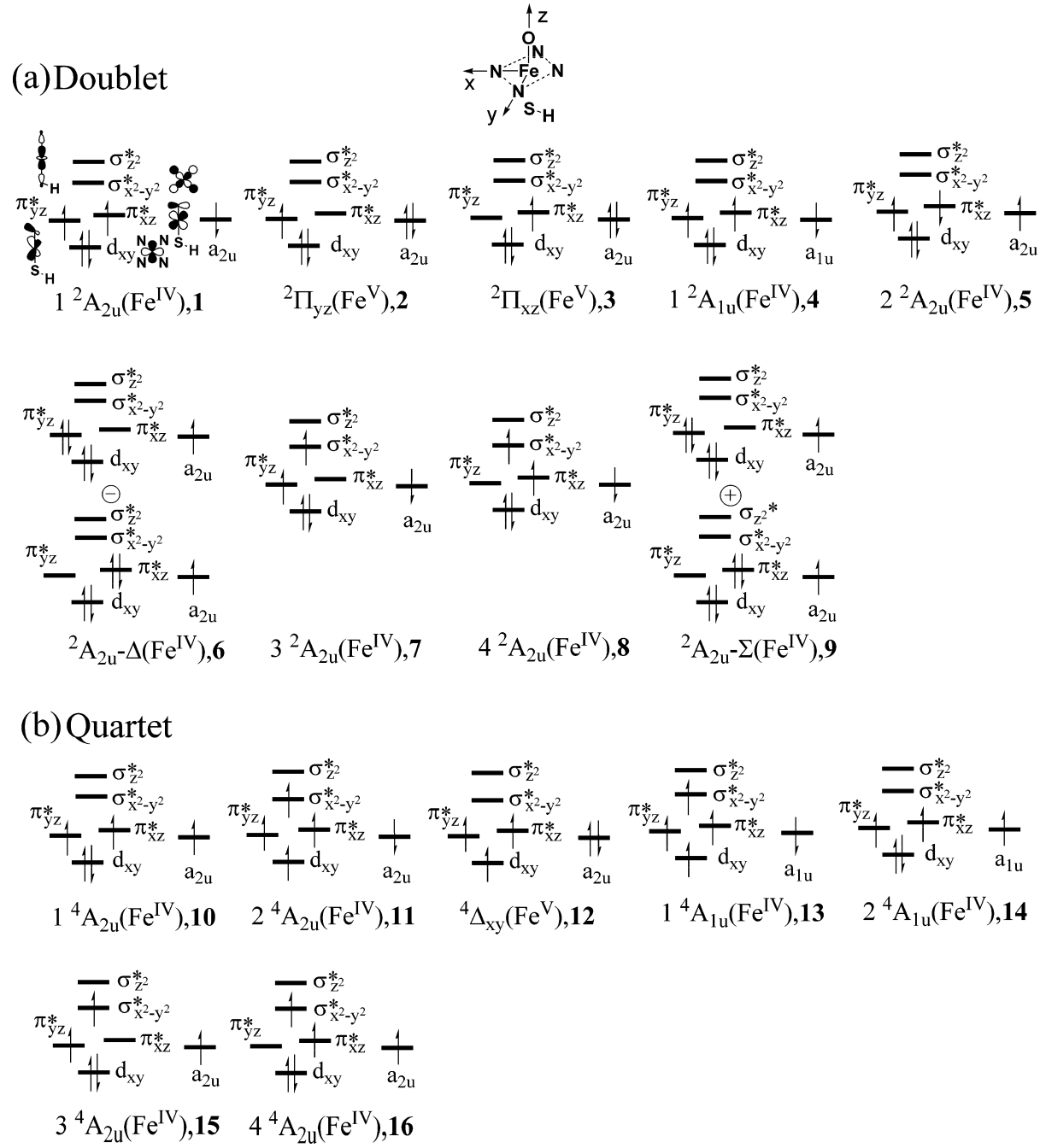


[a] The number in bold after state label is the entry number in Table 2.

mol) to the triradicaloid $Fe^{IV}$ states 1 $^{2,4}A_{2u}(Fe^{IV})$ (**1** and **10**) in energy in both CPO and $P450_{cam}$. We note that there exists also a $^6A_{2u}(Fe^{IV})$ state with a spin-up $a_{2u}$ electron,[8,9,16] which is not computed here. On the basis of the results for the 1 $^{2,4}A_{2u}(Fe^{IV})$ and previous DFT and DFT/MM calculations,[8,9,16] this sextet pentaradicaloid state will lie slightly higher than the quartet state, **11**.

As seen from Scheme 2, the pentaradicaloid $Fe^{IV}$ state **11** differs from the triradicaloid state **1** by excitation of one $d_{xy}$ electron to Fe−N antibonding $\sigma^*_{x^2-y^2}$ orbital. The gap between state **11** and **1** is smaller than the ones provided by the B3LYP/MM calculation of CPO and $P450_{cam}$ where vertical gaps from the ground doublet $Fe^{IV}$ state to this state are both calculated to be about 14−15 kcal/mol at the B3LYP(B2)/MM level. We also tried the recently developed double hybrid functional B2-PLYP,[42] which showed very promising results for improvement of the B3LYP functional in previous extensive calibration calculations.[43] Using a split-valence triple-ζ polarized level basis set (Def2-TZVP[44]), the B2-PLYP/MM calculated vertical gap of 16.9 kcal/mol, between the pentaradicaloid state and triradicaloid state, is close to the B3LYP/MM results in $P450_{cam}$. Thus, CASPT2/MM gives a substantially lower gap than any DFT(functional)/MM method that we tested. In fact, CASPT2/MM

***Scheme 3.*** Schematic Representation of Orbital Occupancies of Main Electronic Configuration of Sulfur Orbital Triradicaloid States of Cpd I Calculated in Table 5[a]

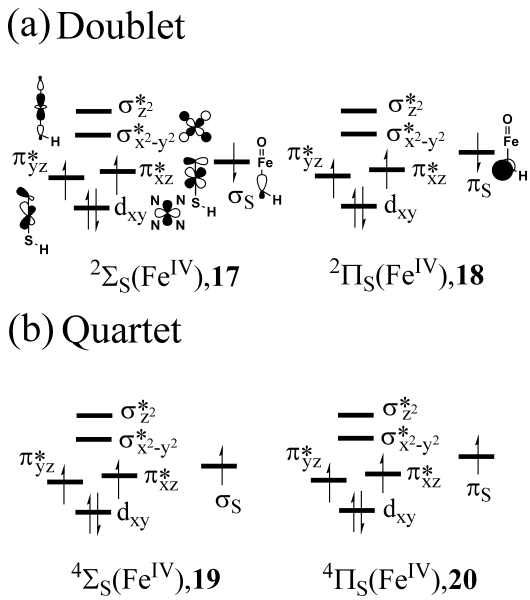


[a] The number in bold after state label is the entry number in Table 5.

***Table 1.*** DFT/MM Calculated and Experimental Key Bond Distances (Å) of the Cpd I Species of CPO and $P450_{cam}$

| | B3LYP/MM[a] | | | exptl[b] | | |
|---|---|---|---|---|---|---|
| enzyme | Fe−O | Fe−$N_{eq}$[c] | Fe−S | Fe−O | Fe−$N_{eq}$[c] | Fe−S |
| CPO | 1.652 | 2.026 | 2.571 | 1.65 | 2.01 | 2.48 |
| $P450_{cam}$ | 1.652 | 2.032 | 2.515 | | | |

[a] B1 used for geometry optimization. [b] Ref 38, no experimental data for $P450_{cam}$ are available. [c] Averaged value for four equatorial Fe−N bonds.

predicts that the pentaradicaloid state for P450 is actually the lowest lying state. However, we must note that the original zero-order Hamiltonian of CASPT2 is known to overestimate the stability of states with more unpaired electrons.[35b] The current zero-order Hamiltonian (IPEA shift = 0.25) used here, designed to minimize this deficiency, has been obtained from a fitting of CASPT2 calculations for some small molecule vis-à-vis experimental data,[35a] and one cannot exclude the possibility that it still favors the pentaradicaloid state over the triradicaloid state for Cpd I.[45] Thus, due to the accuracy limit of the CASPT2 method (about 0.2−0.3 eV) and the proximity of the two states, we still cannot determine the accurate gap between the pentaradicaloid $Fe^{IV}$ quartet state **11** and the ground doublet triradicaloid $Fe^{IV}$ state **1**. What we can deduce from the results is that **11** may be closer to **1** than the DFT/MM datum. We note that previous ab initio multireference correlated treatments for other nonheme iron-oxo species also gave a similar energetic proximity of corresponding $S = 1$ and $S = 2$ ferryl units.[8,17]

***Table 3.*** The Mulliken Charges of $Fe^V$ and $Fe^{IV}$ States Calculated at the CASPT2/MM Level for Cpd I of $P450_{cam}$

| | | Mulliken charge | | | |
|---|---|---|---|---|---|
| state | entry | Fe | O | Por | S |
| 1 $^2A_{2u}(Fe^{IV})$ | **1** | 1.65 | −0.34 | −0.56 | −0.86 |
| $^2\Pi_{yz}(Fe^V)$ | **2** | 1.72 | −0.13 | −0.90 | −0.81 |
| $^4\Delta_{xy}(Fe^V)$ | **12** | 1.78 | −0.19 | −0.87 | −0.84 |

***Table 4.*** The Mulliken Spin Population of Some Low-Lying $Fe^V$ and $Fe^{IV}$ States Calculated at the CASSCF/MM Level for Cpd I of CPO and $P450_{cam}$

| | | CPO | | | | $P450_{cam}$ | | | |
|---|---|---|---|---|---|---|---|---|---|
| state | entry | Fe | O | Por | S | Fe | O | Por | S |
| 1 $^2A_{2u}(Fe^{IV})$ | **1** | 0.76 | 0.59 | −0.33 | −0.02 | 0.77 | 0.57 | −0.33 | −0.01 |
| $^2\Pi_{yz}(Fe^V)$ | **2** | 0.89 | 0.14 | −0.03 | 0.00 | 0.78 | 0.25 | −0.03 | 0.00 |
| $^2\Pi_{xz}(Fe^V)$ | **3** | 0.80 | 0.23 | −0.03 | 0.00 | 0.90 | 0.13 | −0.03 | 0.00 |
| 1 $^4A_{2u}(Fe^{IV})$ | **10** | 1.17 | 0.85 | 0.93 | 0.05 | 1.15 | 0.87 | 0.92 | 0.06 |
| 2 $^4A_{2u}(Fe^{IV})$ | **11** | 3.27 | 0.20 | −0.45 | −0.02 | 3.27 | 0.20 | −0.45 | −0.02 |
| $^4\Delta_{xy}(Fe^V)$ | **12** | 2.09 | 0.99 | −0.08 | 0.00 | 2.11 | 0.98 | −0.09 | 0.00 |

***Table 2.*** CASPT2/MM Relative Energies (kcal/mol), Occupancies of Main Configurations, and Weights (%) of the Main Configurations for Doublet and Quartet States of Cpd I of CPO and $P450_{cam}$ Shown in Scheme 2

| | | CASPT2/MM[a] | | occupancy of main | |
|---|---|---|---|---|---|
| state | entry | CPO | $P450_{cam}$ | configuration | weight (%)[b] |
| 1 $^2A_{2u}(Fe^{IV})$[c] | **1** | 0.0/0.0 | 0.0/0.0 | $(d_{xy})^2(\pi^*_{yz})^1(\pi^*_{xz})^1(\sigma^*_{x^2-y^2})^0(a_{2u})^1$ | 83/83 |
| $^2\Pi_{yz}(Fe^V)$[d] | **2** | 5.6 | 6.0 | $(d_{xy})^2(\pi^*_{yz})^1(\pi^*_{xz})^0(\sigma^*_{x^2-y^2})^0(a_{2u})^2$ | 70/71 |
| $^2\Pi_{xz}(Fe^V)$[d] | **3** | 5.8 | 6.7 | $(d_{xy})^2(\pi^*_{yz})^0(\pi^*_{xz})^1(\sigma^*_{x^2-y^2})^0(a_{2u})^2$ | 70/70 |
| 1 $^2A_{1u}(Fe^{IV})$[d] | **4** | 15.6/17.4 | 17.7/18.8 | $(d_{xy})^2(\pi^*_{yz})^1(\pi^*_{xz})^1(\sigma^*_{x^2-y^2})^0(a_{1u})^1$ | 82/82 |
| 2 $^2A_{2u}(Fe^{IV})$[e] | **5** | 18.3 | 18.4 | $(d_{xy})^2(\pi^*_{yz})^1(\pi^*_{xz})^1(\sigma^*_{x^2-y^2})^0(a_{2u})^1$ | 77/76 |
| $^2A_{2u}-\Delta(Fe^{IV})$[e] | **6** | 19.6 | 19.4 | $(d_{xy})^2(\pi^*_{yz})^2(\pi^*_{xz})^0(\sigma^*_{x^2-y^2})^0(a_{2u})^1 - (d_{xy})^2(\pi^*_{yz})^0(\pi^*_{xz})^2(\sigma^*_{x^2-y^2})^0(a_{2u})^1$ | 77/76 |
| 3 $^2A_{2u}(Fe^{IV})$[e] | **7** | 23.2 | 23.7 | $(d_{xy})^2(\pi^*_{yz})^1(\pi^*_{xz})^0(\sigma^*_{x^2-y^2})^1(a_{2u})^1$ | 66/66 |
| 4 $^2A_{2u}(Fe^{IV})$[e] | **8** | 25.4 | 24.6 | $(d_{xy})^2(\pi^*_{yz})^0(\pi^*_{xz})^1(\sigma^*_{x^2-y^2})^1(a_{2u})^1$ | 64/63 |
| $^2A_{2u}-\Sigma(Fe^{IV})$[e] | **9** | 28.5 | 27.2 | $(d_{xy})^2(\pi^*_{yz})^2(\pi^*_{xz})^0(\sigma^*_{x^2-y^2})^0(a_{2u})^1 + (d_{xy})^2(\pi^*_{yz})^0(\pi^*_{xz})^2(\sigma^*_{x^2-y^2})^0(a_{2u})^1$ | 57/61 |
| 1 $^4A_{2u}(Fe^{IV})$[d] | **10** | 0.9/1.2 | 0.6/0.0 | $(d_{xy})^2(\pi^*_{yz})^1(\pi^*_{xz})^1(\sigma^*_{x^2-y^2})^0(a_{2u})^1$ | 83/83 |
| 2 $^4A_{2u}(Fe^{IV})$[d] | **11** | 0.0 | −1.9 | $(d_{xy})^1(\pi^*_{yz})^1(\pi^*_{xz})^1(\sigma^*_{x^2-y^2})^1(a_{2u})^1$ | 80/80 |
| $^4\Delta_{xy}(Fe^V)$[d] | **12** | 2.2/8.0 | 2.2/7.4 | $(d_{xy})^1(\pi^*_{yz})^1(\pi^*_{xz})^1(\sigma^*_{x^2-y^2})^0(a_{2u})^2$ | 79/78 |
| 1 $^4A_{1u}(Fe^{IV})$[d] | **13** | 15.6 | 16.9 | $(d_{xy})^1(\pi^*_{yz})^1(\pi^*_{xz})^1(\sigma^*_{x^2-y^2})^1(a_{1u})^1$ | 80/80 |
| 2 $^4A_{1u}(Fe^{IV})$[d] | **14** | 17.6/19.8 | 19.2/20.6 | $(d_{xy})^2(\pi^*_{yz})^1(\pi^*_{xz})^1(\sigma^*_{x^2-y^2})^0(a_{1u})^1$ | 83/83 |
| 3 $^4A_{2u}(Fe^{IV})$[e] | **15** | 26.2 | 28.6 | $(d_{xy})^2(\pi^*_{yz})^1(\pi^*_{xz})^0(\sigma^*_{x^2-y^2})^1(a_{2u})^1$ | 65/66 |
| 4 $^4A_{2u}(Fe^{IV})$[e] | **16** | 26.6 | 29.2 | $(d_{xy})^2(\pi^*_{yz})^0(\pi^*_{xz})^1(\sigma^*_{x^2-y^2})^1(a_{2u})^1$ | 65/66 |

[a] The values after the slash are from the original zero-order Hamiltonian (IPEA shift = 0), while the other values (before slash or without slash) are from the standard IPEA zero-order Hamiltonian (IPEA shift = 0.25). [b] Weight of the shown main configuration state functions (CSFs) of CASSCF wave function as represented in Scheme 2, data shown in the CPO/$P450_{cam}$ pattern. [c] This state is taken as the zero of the relative energy scale. [d] Single state calculation. [e] State-average calculation.

***Table 5.*** CASPT2/MM Relative Energies (kcal/mol), Occupancy of Main Configurations, and Weight (%) of the Main Configurations for Four Sulfur-Based Triradicaloid Quartet and Doublet States of Cpd I of CPO and $P450_{cam}$ Shown in Scheme 3

| state | entry | CASPT2/MM[a] CPO | CASPT2/MM[a] $P450_{cam}$ | occupancy of main configuration | weight (%)[b] |
|---|---|---|---|---|---|
| $1\ ^2A_{2u}(Fe^{IV})$[c] | **1** | 0.0 | 0.0 | $(d_{xy})^2(\pi^*_{yz})^1(\pi^*_{xz})^1(\sigma^*_{x^2-y^2})^0(a_{2u})^1(\sigma_S)^2(\pi_S)^2$ | 83/83 |
| $^2\Sigma_S(Fe^{IV})$ | **17** | 14.8 | 26.7 | $(d_{xy})^2(\pi^*_{yz})^1(\pi^*_{xz})^1(\sigma^*_{x^2-y^2})^0(a_{2u})^2(\sigma_S)^1(\pi_S)^2$ | 82/82 |
| $^2\Pi_S(Fe^{IV})$ | **18** | 25.7 | 29.9 | $(d_{xy})^2(\pi^*_{yz})^1(\pi^*_{xz})^1(\sigma^*_{x^2-y^2})^0(a_{2u})^2(\sigma_S)^2(\pi_S)^1$ | 82/82 |
| $^4\Sigma_S(Fe^{IV})$ | **19** | 18.0 | 28.4 | $(d_{xy})^2(\pi^*_{yz})^1(\pi^*_{xz})^1(\sigma^*_{x^2-y^2})^0(a_{2u})^2(\sigma_S)^1(\pi_S)^2$ | 82/82 |
| $^4\Pi_S(Fe^{IV})$ | **20** | 26.5 | 30.6 | $(d_{xy})^2(\pi^*_{yz})^1(\pi^*_{xz})^1(\sigma^*_{x^2-y^2})^0(a_{2u})^2(\sigma_S)^2(\pi_S)^1$ | 82/82 |

[a] The values are from the original zero-order Hamiltonian (IPEA shift = 0) and state-specific calculation. [b] Weight of the shown main CSFs of the CASSCF wave function as represented in Scheme 3, data shown in the CPO/$P450_{cam}$ pattern. [c] This state is taken as zero point in energy.

A technically interesting point is that excluding the "outer" $4d_{xy}$ orbital from the active space leads to overestimation of the stability of state **11** relative to state **1** by about 3 kcal/mol (0.15 eV) and reverses the state ordering. This is the first time that the so-called "double-shell" effect[12] of this $4d_{xy}$ orbital is assessed on the relative energies of the $S = 1$ and $S = 2$ states of ferryl iron-oxo species. The potentially similar effect in the nonheme iron-oxo system remains to be explored.

**C. $Fe^V$ States.** For doublet $Fe^V$ states $^2\Pi_{yz}(Fe^V)$ and $^2\Pi_{xz}(Fe^V)$ (**2**, **3**) and quartet $Fe^V$ state $^4\Delta_{xy}(Fe^V)$ (**12**), our CASPT2/MM calculations turn out also to be quite different from the DFT (B3LYP) or TDDFT/MM results. As reported before, DFT methods converged for the $Fe^V$ state only in the gas phase,[7] but not in a protein environment.[9] In the gas phase, the B3LYP calculations predict that the $Fe^V$ states of Cpd I are about 16−26 kcal/mol higher than the ground state.[7] However, gas phase calculated gaps of the $Fe^V$ to the ground state depend on the used functional and the identity of the axial ligand.[46] Our own exploration of a P450 Cpd I model showed that hybrid functionals predict larger gaps than the GGA functionals, and all the gaps are significant, 15−26 kcal/mol (see Table S5 in the SI). Furthermore, TDDFT/MM in-protein calculations predict an even larger energy gap for the $Fe^V$ state of Cpd I, i.e., more than about 37 for quartet and 46 kcal/mol for doublet states.[9] However, our CASPT2/MM result shows that the standard IPEA zero-order Hamiltonian places the quartet/doublet $Fe^V$ states above the doublet $Fe^{IV}$ ground state in $P450_{cam}$ by only 2.2/6.0 kcal/mol. Interestingly, application of the original CASPT2 zero-order Hamiltonian leads to a somewhat higher gap of 7.4 kcal/mol for the quartet $Fe^V$ state, **12**.[47] So despite the sensitivity of the result to the choice of zero-order Hamiltonian of CASPT2, the calculated CASPT2/MM values are all significantly lower than those from DFT and TDDFT/MM approaches. Interestingly, a recent CASPT2 calculation for chloroiron corrole (Cor) complex shows that, within 1.5 eV of the $Cor^{+\bullet}Fe^{III}Cl$ ground state, there is no high valent $Fe^{IV}$ state in which the corrole ring is closed-shell.[48] This may represent the different tendencies of the corrole and porphyrin ligands to assume a cation radical state.[49]

From the weight of the main configurations shown in last column of Table 2, it can be seen that most of the states, $Fe^V$ included, have dominantly single-configuration characters (70−80%). Thus, the large discrepancy between DFT and CASPT2 based results for these $Fe^V$ states may seem surprising. Nevertheless, we note that this effect is rooted in the large orbital relaxation that attends the CASSCF calculation of Cpd I $Fe^V$ states compared with the $Fe^{IV}$ states. This in turn leads to large stabilization of the $Fe^V$ states in state-specific calculations compared with the state-average calculations at the CASSCF/MM level (the $Fe^V$ states are found to be 32.2−34.9/15.9−18.3 kcal/mol above the triradicaloid ground $Fe^{IV}$ state for state-average/state-specific calculations of CPO, see Tables S6, S7, and S10, Supporting Information). Thus, as exemplified in Figure 2a using a pair of bonding/antibonding orbitals, $\sigma_{x^2-y^2}/\sigma^*_{x^2-y^2}$, the $Fe^V$ state has larger 3d iron components in the Fe−N/Fe−O bonding orbitals $\sigma_{x^2-y^2}/\pi/\sigma_{z^2}$ and smaller 3d components in the Fe−N/Fe−O antibonding $\sigma^*_{x^2-y^2}/\pi^*/\sigma^*_{z^2}$ orbitals, compared with those in the $Fe^{IV}$ state. This different d contribution is caused by the different number of electrons in Fe−O moieties of the $Fe^V$ and $Fe^{IV}$ states, which exerts different screening effects. As shown schematically in Figure 2b, the energy level of the 3d orbitals of iron is lowered in the $Fe^V$ state and thereby affects the first coordinate sphere Fe−O and Fe−N bonding and antibonding orbitals by increasing the contribution of the iron 3d component in the bonding orbitals, while decreasing this contribution to the antibonding orbitals.

Due to this orbital relaxation, which is missing in TDDFT/MM, it is likely that the latter method underestimates the stabilities of the $Fe^V$ states.[50] Indeed, because of the quite different orbitals on iron in the presence of different oxidation states, the state-average treatment in CASSCF/MM calculations for the $Fe^V$ and $Fe^{IV}$ states of Cpd I is also inappropriate. Such a calculation followed by the CASPT2/MM treatment leads to $Fe^V$ states that are substantially lower (by ca. 10 kcal/mol) than the ground $Fe^{IV}$ triradicaloid state **1** (see Table S6−S7 in SI), which we deem to be very unreasonable. Therefore, here we calculated $Fe^{IV}$ and $Fe^V$ states separately to get the most optimal CASSCF orbital set for each state, and hence a balanced CASPT2 treatment. *This finding also cautions against the use of CASSCF state-average treatment for different oxidation states of transition metal containing systems*, especially when the number of states for each metal oxidation state is different, as in the present case. Using our approach, the reference weights of the CASSCF wave functions for the $Fe^V$ and $Fe^{IV}$ states (see Table S10−S11 in SI) in our final CASPT2 wave functions are almost the same, indicating that the treatments for these two states here are balanced.

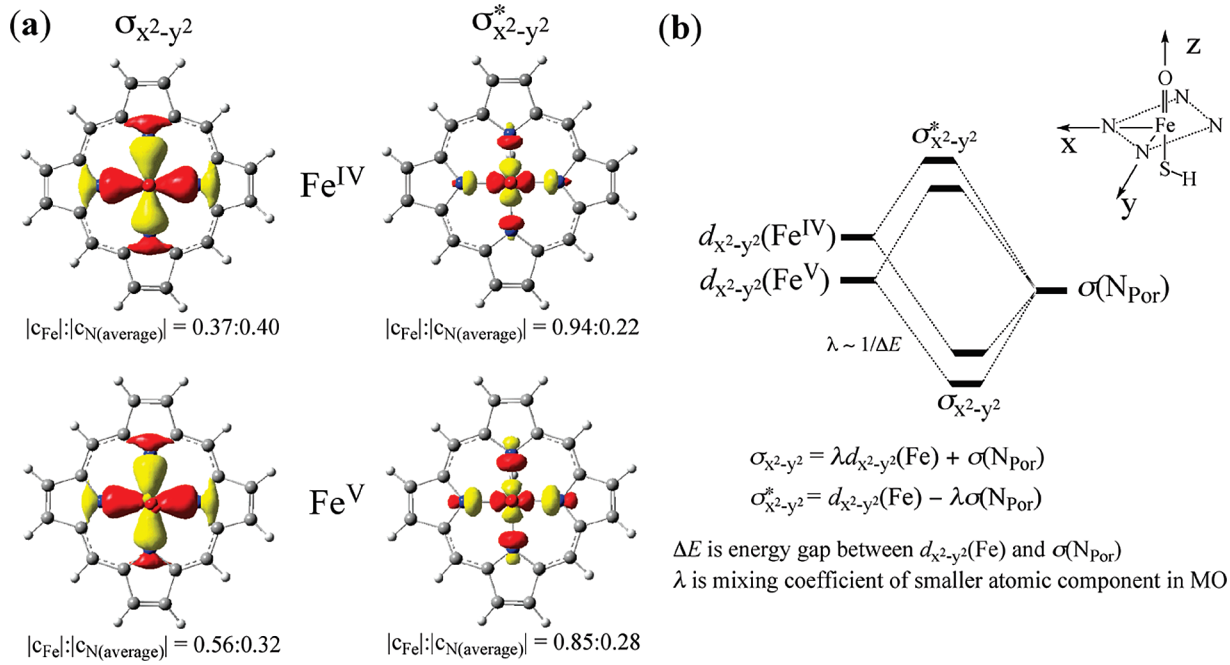


***Figure 2.*** (a) Orbital relaxation of the quartet $Fe^V$ state, $^4\Delta_{xy}(Fe^V)$, compared with the quartet $Fe^{IV}$ state, $1\ ^4A_{2u}(Fe^{IV})$, exemplified by the $\sigma_{x^2-y^2}/\sigma^*_{x^2-y^2}$ bonding/antibonding MOs pair in CPO. The contour value is ±0.05 e/au$^3$. The data underneath the natural orbitals are the ratios of the absolute values of the Fe and N atomic coefficients in a given MO. (b) A schematic representation of effect exerted by the level shift of an iron d orbital on the orbital relaxation.

The calculated Mulliken charges of the doublet and quintet $Fe^V$ states are compared with those of the $Fe^{IV}$ doublet state at the CASPT2/MM level in Table 3. It can be seen that $Fe^V$ states have smaller negative charges on the O atom of the iron-oxo unit, as would be expected from chemical intuition.

In conclusion, although the CASPT2/MM energy gaps of the $Fe^V$ state are quite low, ≤10 kcal/mol, the variance caused by the two choices of zero-order Hamiltonians does not allow a clear-cut determination of the $Fe^V-Fe^{IV}$ gaps. Perhaps, future calculations with other high level ab initio multireference approaches, such as the SORCI method,[51] which could hopefully be applied to the current large system, will give a more definitive answer to this difficult question of how high the $Fe^V$ states are. Taking the present CASPT2/MM results at face value, the $Fe^V$ states appear to be in principle accessible for affecting the reactivity of Cpd I (see discussion below).

**D. Spin Density Distribution in the $Fe^{IV}$ and $Fe^V$ States.** The calculated Mulliken spin populations for some of the lowest states in Table 2 are collected in Table 4. The calculated values for two $Fe^{IV}$ triradicaloid states here are close to the previous multiconfigurational calculations.[13,14] The trend among the other states is physically reasonable and can be deduced from the orbital diagrams in Scheme 2. The absolute value of spin density on the thiolate ligand in the triradicaloid states is small ≤0.06, somewhat smaller than in DFT/MM calculations (0.08−0.16).[19a] By comparison, the experimental spin density[3e] for CPO was determined as being smaller than 0.23. No discussion was given[3e] as to how much smaller than 0.23 the actual number is, and it would be interesting to reconsider the experimental data in light of these computed spin densities.

**E. $^1\Delta_g$ and $^1\Sigma^+_g$ States Analogous to States of $O_2$ and $a_{1u}$ Singly Occupied States.** As has been noted several times,[52] the FeO moiety of Cpd I has states analogous to those of the $O_2$ molecule, namely, the $^1\Delta_g$ and $^1\Sigma^+_g$ states. These states of $^2A_{2u}-\Delta(Fe^{IV})$ (**6**) and $^2A_{2u}-\Sigma(Fe^{IV})$ (**9**; in Scheme 2), which involve mixing of two configurations, each having one doubly occupied $\pi^*$ orbital, are problematic for DFT. We therefore decided to calculate these states as well and find if they are low enough to contribute to the reactivity of Cpd I. As with previous SORCI results for the iron-oxo model complex,[8] our calculated energy gaps (see Table 2) for the doublet states that are analogous to the $^1\Delta_g$ and $^1\Sigma^+_g$ states of the $O_2$ molecule (**6** and **9**) turn out to be quite large, indicating that they are not likely to become relevant in Cpd I involved reactions.[53]

The importance of the $a_{1u}$ singly occupied states has been debated in the literature quite extensively.[54,55] In our calculation with the standard IPEA zero-order Hamiltonian, the $a_{1u}$ singly occupied states $1\ ^2A_{1u}(Fe^{IV})$, $1\ ^4A_{1u}(Fe^{IV})$, and $2\ ^4A_{1u}(Fe^{IV})$ (**4**, **13**, **14**) were located 15.6−16.7/17.7−18.8 kcal/mol higher than the corresponding $a_{2u}$ singly occupied states $1\ ^2A_{2u}(Fe^{IV})$, $2\ ^4A_{2u}(Fe^{IV})$, and $1\ ^4A_{2u}(Fe^{IV})$ (**1**, **11**, **10**) for CPO/$P450_{cam}$. These substantial gaps compared to the $a_{2u}$ states are larger than a very small value of 1.9 kcal/mol obtained at the DDCI2-Q level.[13] Interestingly, the calculated values are comparable with the TDDFT(B3LYP)/MM value of 12.3 kcal/mol for $P450_{cam}$.[13] In contrast to the $Fe^V$ states above, for the $a_{1u}$ singly occupied state, we do not observe large orbital relaxation phenomenon compared with the $a_{2u}$ singly occupied state; hence the TDDFT results for this state may be more reliable than that for $Fe^V$ states. As observed before,[13,14,56] we notice that the $a_{2u}$ singly occupied states are lower than the corresponding $a_{1u}$ singly occupied states

because of dynamic correlation. Indeed, at the CASSCF/MM level, their energetic levels are reversed compared with the CASPT2/MM situation. As can be seen from Table 2, in contrast to the $Fe^V$ states, the sensitivity of the $A_{1u}$ state energies to the choice of zero-order Hamiltonian of CASPT2 is not significant.

**F. Sulfur-Based Radicaloid States.** The sulfur-based triradicaloid quartet and doublet states $^{2,4}\Sigma_S(Fe^{IV})$ and $^{2,4}\Pi_S(Fe^{IV})$ shown in Scheme 3, in which the singly occupied porphyrin $a_{2u}$ orbital of the $A_{2u}$ ground states is replaced by singly occupied sulfur $\sigma_S$ and $\pi_S$ orbitals, respectively, were found to be very low lying in previous gas phase DFT calculations.[7,57−59] In some cases, depending on the thiolate ligand representation ($SCH_3$ instead of SH), these sulfur radical states came out as the ground states, and the protein environment was needed to retrieve the $A_{2u}$ ground states.[58] We therefore decided to explore their energy levels using CASPT2/MM calculations. The states are shown in Scheme 3, while the relative energies are collected in Table 5.

Similarly to the case of $Fe^V$ states, here too the state-average orbitals are far from being optimal for the $A_{2u}$ and $\Sigma_S/\Pi_S$ states at the same time. Large CASSCF(15,14) calculations (see Table S8 in SI) that include either $a_{2u}$ and one of two sulfur orbitals or two sulfur orbitals in the active space indicate that the $A_{2u}$ state and $\Sigma_S/\Pi_S$ state can be calculated separately in active spaces excluding the nearly doubly occupied $\sigma_S/\pi_S$ orbital and $a_{2u}$ orbital (with occupancies >1.999), respectively. So we used such a state-specific strategy to calculate one state in each calculation. The results for these states show (see SI for details) that they are at least 14.8 kcal/mol higher above the ground doublet state **1** for CPO at the CASPT2/MM level.[60] This value is higher than the corresponding lowest result (9.6 kcal/mol) of the previous CASPT2 gas phase calculation,[14] clearly indicating that the protein environment causes the sulfur-based triradicaloid state to be less favored than the porphyrin-based triradicaloid state of Cpd I. Another interesting difference between CASPT2 gas phase and CASPT2/MM calculations for the $\Sigma_S/\Pi_S$ state is that our CASPT2/MM calculation predicts that the former state is lower in energy than the latter, while in the gas phase the state ordering is opposite. This difference may be caused by the larger stabilization of the $\pi_S$ orbital compared with the $\sigma_S$ orbital, due to interactions with the protein environment caused by the different orbital directionalities. The main stabilizing factor for the $\sigma_S$ orbital comes from the iron ion and it is present in the gas phase already, while for the $\pi_S$ orbital, the protein may have additional stabilization through an amidic hydrogen-bonding-type interaction (NH···S) between the sulfur atom and the peptide bonds (HN−CO) of the proximal residues around the proximal cysteine ligand. We note that these sulfur-based radicaloid states were predicted to be 60−70 kcal/mol lower than the $a_{2u}$ triradicaloid state at the CASSCF level in the previous gas phase calculation,[14] but here within the protein environment, the sulfur and $a_{2u}$ triradicaloid states of Cpd I are already comparable at the CASSCF/MM level, in accord with previous analysis.[7] This situation in protein makes the multistate strategy less crucial here than that in the gas phase (see Table S9 in SI).[14]

Another noteworthy feature in Table 5 is that the differences between the corresponding relative energies of sulfur-based triradicaloid states of CPO and $P450_{cam}$ are quite large, which is in contrast with the similar state gaps for the other states in Table 2. The gaps in CPO are significantly smaller than the corresponding ones in $P450_{cam}$, especially for the $\Sigma_S$ state. This result indicates that the relative stability of sulfur-based triradicaloid states can be quite enzyme-dependent. It is generally accepted that CPO has a more polar pocket than the one possessed by $P450_{cam}$,[1,2] which was also confirmed by the previous QM/MM analysis.[19a] But our results show that at least for the region near the sulfur atom, the accumulation of the negative charges on S in state **1** compared with the sulfur-based triradicaloid states (**17**−**20**) is less favored energetically in CPO than that in $P450_{cam}$. This result is quite surprising since it is usually considered that the polar environment should generally favor the electronic state with more charge separation and localization. The most probable explanation for these very different relative energies of the $\Sigma_S$ states in the two enzymes could be due to the Fe−S bond distance, which is about 0.06 Å shorter in $P450_{cam}$ than that in CPO at the QM/MM level. This shorter bond stabilizes the $\sigma_S$ orbital of S (but less for $\pi_S$) and thereby increases the corresponding state energy gap for $P450_{cam}$.

**G. A Brief Discussion on the Potential Impact of the Cpd I States on Reactivity.** The above CASPT2/MM results reveal that Cpd I is a remarkable reagent having more than 20 states jammed within 30 kcal/mol. Considering that the computed barriers for H abstraction range between 6−23 kcal/mol,[1g] depending on the substrate, it might be expected that many of the states will contribute to the reactivity of Cpd I by affecting the transition state character, and some may even be involved directly. In this last respect, CASPT2/MM shows that in addition to the consensual triradicaloid states, $1\ ^{2,4}A_{2u}(Fe^{IV})$, there may be four additional low-lying states. These are the pentaradicaloid, $2\ ^4A_{2u}(Fe^{IV})$, and the perferryls, $^2\Pi_{yz/xz}(Fe^V)$ and $^4\Delta_{xy}(Fe^V)$. In the $^6A_{2u}(Fe^{IV})$ state (not calculated in this work), the $a_{2u}$ radical being ferromagnetically coupled with a $S = 2$ Fe−O ferryl unit should also be close in energy to the pentaradicaloid $2\ ^4A_{2u}(Fe^{IV})$ state. We cannot say with certainty that the CASPT2/MM energy gaps are converged with respect to the active space and basis set used, but if we take the present results at their face values, then the energy gaps of the perferryl and pentaradicaloid states relative to the $1\ ^{2,4}A_{2u}(Fe^{IV})$ states are well below most of the barriers calculated so far for the triradicaloid states.[1f,g] One should then consider that the pentaradicaloid and perferryl states should be energetically available along the reaction pathways of Cpd I. In such a putative scenario, if the crossover probabilities from the triradicaloid to the pentaradicaloid and perferryl states were nonzero, these latter states, being so low in energy and perhaps also possessing small barriers, would have led to MSR and brought about a significant enhancement of reactivities of the P450 and CPO Cpd I species. However, with one exception in model systems,[10] all the other LFP generated Cpd I species of P450 and synthetic models are reactive but not overwhelmingly so.[6] *This suggests that there are no additional low-lying*

***Scheme 4.*** Schematic Representation of Increase of the Exchange Interaction during Electron Redistribution in Hydrogen Abstraction of C−H Bond by Quartet Pentaradicaloid State

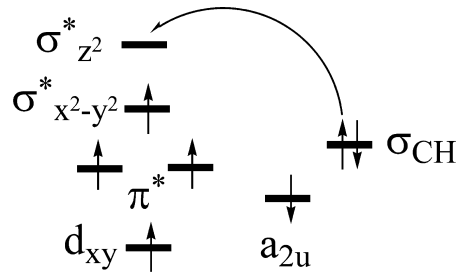


*states that participate in a direct way in the normal reactivity nascent from the 1 $^{2,4}A_{2u}(Fe^{IV})$ states*. However, if the present CASPT2/MM results are reliable, then the $Fe^{V}$ and the 2 $^{4}A_{2u}(Fe^{IV})$ states may affect reactivity if they could be accessed directly, as suggested in recent papers for the perferryl states.[6,18] Will these state-specific reactions indeed be so much faster than the ground state's reaction? This is still a question. Let us then discuss some prospective features of these state-specific reactivities.

*Reactivity Patterns of the Pentaradicaloid States.* As seen from the main configuration of the pentaradicaloid state (Scheme 2), the number of unpaired electrons on iron-centered orbitals changes from 2 to 4 compared with the triradicaloid state **1**. This brings more exchange interaction for the pentaradicaloid state relative to the triradicaloid states[16] and counteracts the orbital gap due to the $d_{xy}$ to $\sigma^*_{x^2-y^2}$ excitation. This effect increases along the oxidation pathway. Thus, as shown in Scheme 4, for example, during the hydroxylation reaction by the pentaradicaloid state of Cpd I, the number of unpaired electrons on iron increases to five, and hence increasing the number of exchange correlation interactions lowers the hydrogen abstraction barrier from this state relative to the triradicaloid state. Although this is counteracted to some extent by the orbital energy gap, associated with the $a_{2u}\rightarrow\sigma^*_{z^2}$ electron shift, the exchange stabilization wins out and leads to a net stabilization; hence, the pentaradicaloid states would be typified by *exchange-enhanced reactivity*.

The DFT[16] and DFT/MM[9] calculation have shown that hydrogen abstraction barrier on the $Fe^{IV}$ pentaradicaloid state is indeed much lower than that on the $Fe^{IV}$ triradicaloid state. Given the fact that CASPT2/MM predicts the energy of the 2 $^{4}A_{2u}(Fe^{IV})$ state to be virtually degenerate with the ground state, even if its stability is overestimated, the impact of this state on the reactivity of Cpd I has to be seriously considered. We note that a similar conclusion has been reached from DFT/MM and DFT calculations, namely, that, even at these levels, the involvement of the pentaradicaloid states in reactivity is a likely event.[9,16] However, with the exception of a recent tentative suggestion by Groves,[10] there are no experimental data or methods that enable evaluation of the potential contribution of the pentaradicaloid channel to reactivity. Reconsideration of the effect of the pentaradicaloid states on the spectroscopy (e.g., Mössbauer) of the triradicaloid ground state may assist the evaluation of the energy gap between the states.

*Reactivity of the Perferryl States.* Turning now to the $Fe^{V}$═O states, we note that reactivities of $Fe^{V}$═O as well as of $Fe^{IV}$═O reagents have been studied in the nonheme complexes.[61−72] However, the reactivity of the only characterized perferryl reagent[64] seems to be inferior compared with the most reactive ferryl reagents like [BnTPEN-$Fe^{IV}$(O)$(O_3SCF_3)]^+$ (BnTPEN, *N*-benzyl-*N*,*N*′,*N*′-tris(2-pyridylmethyl)-1,2-diaminoethane) which can even activate an inert C−H bond like in cyclohexane.[72] In contrast, the reactivity of the putative perferryl reagents, of the $L_4Fe^{V}$(O)(OH) types, is indeed higher than that of ferryl reagents,[61−63] but since these perferryl complexes have not been characterized, one may question whether or not the experimental trend actually reflects intrinsic perferryl reactivity. Very high reactivity has been reported for the PorMn$^{V}$O reagents.[73] However, as was argued by Groves[73a] and demonstrated computationally by Groves-Car et al.,[74] Eisenstein et al.,[75] and one of us,[76] the high reactivity of these reagents is due to TSR (two-state reactivity) and involves the higher spin states of these reagents.

In summary, before drawing any conclusions on the putative reactivity of the $Fe^{V}$ and pentaradicaloid states of P450, one would have to ascertain (e.g., by CASPT2/MM) that such state specific reactions are indeed faster than those nascent from the 1 $^{2,4}A_{2u}(Fe^{IV})$ ground states.

## Conclusions

The ab initio multireference correlated QM/MM treatment for an open-shell transition-metal-containing biochemical system is highly complex and requires considerable insight and technical control and hence has not been widely used compared with the DFT/MM approach in computational bioinorganic chemistry.[77] However, the increasing number of applications of ab initio multireference correlated methods recently in transition metal containing molecules[8,13,14,17,48,78−92] is naturally leading also to applications in the complex field of metalloenzyme systems. In this work, we performed high level ab initio multireference correlated CASPT2/MM calculations to assess the low-lying states of the important reactive species Cpd I in $P450_{cam}$ and CPO, at a significantly advanced level of state completeness, overlaid with the protein environment effects. This is achieved by using a large active space with all the iron 3d orbitals and some 4d involved orbitals to account for the double-shell effect. Similar with a previous CASSCF/MM application to the oxyheme species in myoglobin,[93] the current CASPT2/MM treatment for the Cpd I system is different in many aspects from the gas phase CASPT2 treatment. This difference underscores the influence of the protein environment on the state description and energy levels in these electron deficient systems. In this respect, *the CASPT2/MM study shows that DFT/MM results are reliable for many of the states studied here*, and with the notable exception of the pentaradicaloid and perferryl states, there is by and large a reasonably good accord between DFT/MM and CASPT2/MM.

The CASPT2/MM calculations predict that in Cpd I in addition to the two nearly degenerate $Fe^{IV}$ quartet and doublet triradicaloid states, as revealed by DFT and DFT/MM methods, both $Fe^{IV}$ pentaradicaloid and $Fe^{V}$ states *are*

*possibly accessible in energy*. This raises questions whether the $Fe^{V}$ states or $Fe^{IV}$ pentaradicaloid states of Cpd I could contribute directly to the reactivity of Cpd I of P450. Previous DFT/MM calculations suggested that the hydrogen abstraction barrier on the $Fe^{IV}$ pentaradicaloid state is lower than that on the $Fe^{IV}$ triradicaloid state.[9] If these states are really involved in reactions of Cpd I, then a multistate reactivity, rather than the two-state reactivity suggested before,[94] would necessarily become a minimal and a better model to understand Cpd I reactivity in P450. A better assessment of this feature can, however, be made only after ascertaining that the present CASPT2/MM state gaps are converged with respect to increasing the active space and basis set, and by estimation of the barriers of reactions catalyzed by P450 such as hydroxylation at the CASPT2/MM level. Studies along these lines are under way in our research group.

**Acknowledgment.** We thank Prof. B. O. Roos for helpful discussions. S.S. is supported by an ISF grant (53/09). H.C. thanks the Golda Meir fellowship fund. J.S.S. thanks the financial support from the China Scholarship Council (CSC). W.W. is supported by the Natural Science Foundation of China (No 20533020, 20873106).

**Supporting Information Available:** Computational procedures and a full set of computational results. This material is available free of charge via the Internet at http://pubs.acs.org.

## References

(1) (a) Omura, T.; Sato, R. *J. Biol. Chem.* **1962**, *237*, 1375–1376. (b) Sono, M.; Roach, M. P.; Coulter, E. D.; Dawson, J. H. *Chem. Rev.* **1996**, *96*, 2841–2887. (c) Denisov, I. G.; Makris, T. M.; Sligar, S. G.; Schlichting, I. *Chem. Rev.* **2005**, *105*, 2253–2277. (d) Ortiz de Montellano, P. R. *Cytochrome P450: Structure, Mechanism and Biochemistry*, 3rd ed.; Kluwer Academic/Plenum: New York, 2005. (e) Meunier, B.; de Visser, S. P.; Shaik, S. *Chem. Rev.* **2005**, *104*, 3947–3980. (f) Shaik, S.; Kumar, D.; de Visser, S. P.; Altun, A.; Thiel, W. *Chem. Rev.* **2005**, *105*, 2279–2328. (g) Shaik, S.; Cohen, S.; Wang, Y.; Chen, H.; Kumar, D.; Thiel, W. *Chem. Rev.* **2010**, *110*, 947–1017.

(2) (a) Morris, D. R.; Hager, L. P. *J. Biol. Chem.* **1966**, *241*, 1763–1768. (b) Dawson, J. H.; Sono, M. *Chem. Rev.* **1987**, *87*, 1255–1276. (c) Sundaramoorthy, M. Chloroperoxidase. In *Handbook of Metalloproteins*; Messerschmidt, A., Huber, R., Poulos, T. L., Wieghardt, K., Eds.; John-Wiley and Sons: New York, 2001; Vol. 1, pp 233−244.

(3) (a) Rutter, R.; Hager, L. P.; Dhonau, H.; Hendrich, M.; Valentine, M.; Debrunner, P. *Biochemistry* **1984**, *23*, 6809–6816. (b) Palcic, M. M.; Rutter, R.; Araiso, T.; Hager, L. P.; Dunford, H. B. *Biochem. Biophys. Res. Commun.* **1980**, *94*, 1123–1127. (c) Egawa, T.; Proshlyakov, D. A.; Miki, H.; Makino, R.; Ogura, T.; Kitagawa, T.; Ishimura, Y. *J. Biol. Inorg. Chem.* **2001**, *6*, 46–54. (d) Hosten, C. M.; Sullivan, A. M.; Palaniappan, V.; Fitzgerald, M. M.; Terner, J. *J. Biol. Chem.* **1994**, *269*, 13966–13978. (e) Kim, S. H.; Perera, R.; Hager, L. P.; Dawson, J. H.; Hoffman, B. M. *J. Am. Chem. Soc.* **2006**, *128*, 5598–5599. (f) Stone, K. L.; Behan, R. K.; Green, M. T. *Proc. Natl. Acad. Sci. U.S.A.* **2006**, *103*, 12307–12310.

(4) (a) Davydov, R.; Makris, T. M.; Kofman, V.; Werst, D. E.; Sligar, S. G.; Hoffman, B. M. *J. Am. Chem. Soc.* **2001**, *123*, 1403–1415. (b) Denisov, I. G.; Makris, T. M.; Sligar, S. G. *J. Biol. Chem.* **2001**, *276*, 11648–11652.

(5) (a) Egawa, T.; Shimada, H.; Ishimura, Y. *Biochem. Biophys. Res. Commun.* **1994**, *201*, 1464–1469. (b) Spolitak, T.; Dawson, J. H.; Ballou, D. P. *J. Biol. Chem.* **2005**, *280*, 20300–20309. (c) Kellner, D. G.; Hung, S. C.; Weiss, K. E.; Sligar, S. G. *J. Biol. Chem.* **2002**, *277*, 9641–9644.

(6) (a) Sheng, X.; Horner, J. H.; Newcomb, M. *J. Am. Chem. Soc.* **2008**, *130*, 13310–13320. (b) Sheng, X.; Zhang, H. M.; Im, S.-C.; Horner, J. H.; Waskell, L.; Hollenberg, P. F.; Newcomb, M. *J. Am. Chem. Soc.* **2009**, *131*, 2971–2976. (c) Wang, Q.; Sheng, X.; Horner, J. H.; Newcomb, M. *J. Am. Chem. Soc.* **2009**, *131*, 10629–10636.

(7) Ogliaro, F.; de Visser, S. P.; Groves, J. T. *Angew. Chem., Int. Ed.* **2001**, *40*, 2874–2878.

(8) Schöneboom, J. C.; Neese, F.; Thiel, W. *J. Am. Chem. Soc.* **2005**, *127*, 5840–5853.

(9) Altun, A.; Shaik, S.; Thiel, W. *J. Am. Chem. Soc.* **2007**, *129*, 8978–8987.

(10) Bell, S. R.; Groves, J. T. *J. Am. Chem. Soc.* **2009**, *131*, 9640–9641.

(11) (a) Schöneboom, J. C.; Lin, H.; Reuter, N.; Thiel, W.; Cohen, S.; Ogliaro, F.; Shaik, S. *J. Am. Chem. Soc.* **2002**, *124*, 8142–8151. (b) Schöneboom, J. C.; Cohen, S.; Lin, H.; Shaik, S.; Thiel, W. *J. Am. Chem. Soc.* **2004**, *126*, 4017–4034. (c) Bathelt, C. M.; Zurek, J.; Mulholland, A. J.; Harvey, J. N. *J. Am. Chem. Soc.* **2005**, *127*, 12900–12908. (d) Guallar, V.; Baik, M.-H.; Lippard, S. J.; Friesner, R. *Proc. Natl. Acad. Sci. U.S.A.* **2003**, *100*, 6998–7002. (e) Guallar, V.; Friesner, R. *J. Am. Chem. Soc.* **2004**, *126*, 8501–8508.

(12) Roos, B. O.; Andersson, K.; Fülscher, M. P.; Malmqvist, P.-Å.; Serrano-Andrés, L.; Pierloot, K.; Merchán, M. *Adv. Chem. Phys.* **1996**, *43*, 219–331.

(13) Altun, A.; Kumar, D.; Neese, F.; Thiel, W. *J. Phys. Chem. A* **2008**, *112*, 12904–12910.

(14) Radoń, M.; Broclawik, E. *J. Chem. Theory Comput.* **2007**, *3*, 728–734.

(15) (a) Green, M. T. *J. Am. Chem. Soc.* **1999**, *121*, 7939–7940. (b) Ogliaro, F.; Cohen, S.; de Visser, S. P.; Shaik, S. *J. Am. Chem. Soc.* **2000**, *122*, 12892–12893.

(16) Hirao, H.; Kumar, D.; Thiel, W.; Shaik, S. *J. Am. Chem. Soc.* **2005**, *127*, 13007–13018.

(17) (a) Neese, F. *J. Inorg. Biochem.* **2006**, *100*, 716–726. (b) Berry, J. F.; DeBeer George, S.; Neese, F. *Phys. Chem. Chem. Phys.* **2008**, *10*, 4361–4374.

(18) (a) Newcomb, M.; Zhang, R.; Chandrasena, R. E.; Halgrimson, J. A.; Horner, J. H.; Makris, T. M.; Sligar, S. G. *J. Am. Chem. Soc.* **2006**, *128*, 4580–4581. (b) Pan, Z. Z.; Zhang, R.; Fung, L. W.-M.; Newcomb, M. *Inorg. Chem.* **2007**, *46*, 1517–1519. (c) Pan, Z. Z.; Wang, Q.; Sheng, X.; Horner, J. H.; Newcomb, M. *J. Am. Chem. Soc.* **2009**, *131*, 2621–2628. (d) Harischandra, D. N.; Zhang, R.; Newcomb, M. *J. Am. Chem. Soc.* **2005**, *127*, 13776–13777. (e) Watanabe, Y. *J. Biol. Inorg. Chem.* **2001**, *6*, 846–856. (f) Nanthakumar, A.; Goff, H. M. *J. Am. Chem. Soc.* **1990**, *112*, 4047–4049.

(19) (a) Cho, K.-B.; Hirao, H.; Chen, H.; Carvajal, M. A.; Cohen, S.; Derat, E.; Thiel, W.; Shaik, S. *J. Phys. Chem. A* **2008**, *112*, 13128–13138. (b) Lai, W. Z.; Chen, H.; Shaik, S. *J. Phys. Chem. B* **2009**, *113*, 7912–7917. (c) Chen, H.; Hirao, H.; Derat, E.; Schlichting, I.; Shaik, S. *J. Phys. Chem. B* **2009**, *112*, 9490–9500.

(20) Sherwood, P.; de Vries, A. H.; Guest, M. F.; Schreckenbach, G.; Catlow, C. R. A.; French, S. A.; Sokol, A. A.; Bromley, S. T.; Thiel, W.; Turner, A. J.; Billeter, S.; Terstegen, F.; Thiel, S.; Kendrick, J.; Rogers, S. C.; Casci, J.; Watson, M.; King, F.; Karlsen, E.; Sjøvoll, M.; Fahmi, A.; Schäfer, A.; Lennartz, C. *J. Mol. Struct. (THEOCHEM)* **2003**, *632*, 1–28.

(21) Ahlrichs, R.; Bär, M.; Häser, M.; Horn, H.; Kölmel, C. *Chem. Phys. Lett.* **1989**, *162*, 165–169.

(22) Smith, W.; Forester, T. R. *J. Mol. Graphics* **1996**, *14*, 136–141.

(23) (a) Becke, A. D. *Phys. Rev. A* **1988**, *38*, 3098–3100. (b) Lee, C.; Yang, W. T.; Parr, R. G. *Phys. Rev. B* **1988**, *37*, 785–789. (c) Becke, A. D. *J. Chem. Phys.* **1993**, *98*, 5648–5652. (d) Becke, A. D. *J. Chem. Phys.* **1993**, *98*, 1372–1377.

(24) Mackerell, A. D., Jr.; Bashford, D.; Bellott, M.; Dunbrack, R. L., Jr.; Evanseck, J. D.; Field, M. J.; Fischer, S.; Gao, J.; Guo, H.; Ha, S.; Joseph-McCarthy, D.; Kuchnir, L.; Kuczera, K.; Lau, F. T. K.; Mattos, C.; Michnick, S.; Ngo, T.; Nguyen, D. T.; Prodhom, B.; Reiher, W. E., III; Roux, B.; Schlenkrich, M.; Smith, J. C.; Stote, R.; Straub, J.; Watanabe, M.; Wiórkiewicz-Kuczera, J.; Yin, D.; Karplus, M. *J. Phys. Chem. B* **1998**, *102*, 3586–3616.

(25) Hay, P. J.; Wadt, W. R. *J. Chem. Phys.* **1985**, *82*, 299–310.

(26) (a) Wachters, A. J. H. *J. Chem. Phys.* **1970**, *52*, 1033–1036. (b) Hay, P. J. *J. Chem. Phys.* **1977**, *66*, 4377–4384. (c) Bauschlicher, C. W., Jr.; Langhoff, S. R.; Partridge, H.; Barnes, L. A. *J. Chem. Phys.* **1989**, *91*, 2399–2411. (d) Stewart, R. F. *J. Chem. Phys.* **1970**, *52*, 431–438.

(27) Hehre, W. J.; Ditchfield, R.; Pople, J. A. *J. Chem. Phys.* **1972**, *56*, 2257–2261.

(28) (a) Bakowies, D.; Thiel, W. *J. Phys. Chem.* **1996**, *100*, 10580–10594. (b) de Vries, A. H.; Sherwood, P.; Collins, S. J.; Rigby, A. M.; Rigutto, M.; Kramer, G. J. *J. Phys. Chem. B* **1999**, *103*, 6133–6141. (c) Sherwood, P.; de Vries, A. H.; Collins, S. J.; Greatbanks, S. P.; Burton, N. A.; Vincent, M. A.; Hillier, I. H. *Faraday Discuss.* **1997**, *106*, 79–92.

(29) Billeter, S. R.; Turner, A. J.; Thiel, W. *Phys. Chem. Chem. Phys.* **2000**, *2*, 2177–2186.

(30) Karlström, G.; Lindh, R.; Malmqvist, P.-Å.; Roos, B. O.; Ryde, U.; Veryazov, V.; Widmark, P.-O.; Cossi, M.; Schimmelpfennig, B.; Neogrady, P.; Seijo, L. *Comput. Mater. Sci.* **2003**, *28*, 222–239.

(31) (a) Douglas, M.; Kroll, N. M. *Ann. Phys.* **1974**, *82*, 89–155. (b) Hess, B. A. *Phys. Rev. A* **1986**, *33*, 3742–3748.

(32) Balabanov, N. B.; Peterson, K. A. *J. Chem. Phys.* **2005**, *123*, 064107/1−064107/15.

(33) de Jong, W. A.; Harrison, R. J.; Dixon, D. A. *J. Chem. Phys.* **2001**, *114*, 48–53.

(34) Aquilante, F.; Malmqvist, P.-Å.; Pedersen, T. B.; Ghosh, A.; Roos, B. O. *J. Chem. Theory Comput.* **2008**, *4*, 694–702.

(35) (a) Ghigo, G.; Roos, B. O.; Malmqvist, P.-Å. *Chem. Phys. Lett.* **2004**, *396*, 142–149. (b) Andersson, K.; Roos, B. O. *Int. J. Quantum Chem.* **1993**, *45*, 591–607.

(36) Finley, J.; Malmqvist, P.-Å.; Roos, B. O.; Serrano-Andrés, L. *Chem. Phys. Lett.* **1998**, *288*, 299–306.

(37) Forsberg, N.; Malmqvist, P.-Å. *Chem. Phys. Lett.* **1997**, *274*, 196–204.

(38) Stone, K. L.; Behan, R. K.; Green, M. T. *Proc. Natl. Acad. Sci. U.S.A.* **2005**, *102*, 16563–16565.

(39) de Visser, S. P.; Ogliaro, F.; Harris, N.; Shaik, S. *J. Am. Chem. Soc.* **2001**, *123*, 3037–3047.

(40) Hirao, H.; Kumar, D.; Que, L., Jr.; Shaik, S. *J. Am. Chem. Soc.* **2006**, *128*, 8590–8606.

(41) (a) Shaik, S.; Kumar, D.; de Visser, S. P. *J. Am. Chem. Soc.* **2008**, *130*, 10128–10140. (b) de Visser, S. P.; Kumar, D.; Cohen, S.; Shacham, R.; Shaik, S. *J. Am. Chem. Soc.* **2004**, *126*, 8362–8363.

(42) Grimme, S. *J. Chem. Phys.* **2006**, *124*, 034108/1−034116/16.

(43) (a) Schwabe, T.; Grimme, S. *Phys. Chem. Chem. Phys.* **2006**, *8*, 4398–4401. (b) Neese, F.; Schwabe, T.; Grimme, S. *J. Chem. Phys.* **2007**, *126*, 124115/1–034116/15. (c) Schwabe, T.; Grimme, S. *Acc. Chem. Res.* **2009**, *41*, 569–579.

(44) Schäfer, A.; Huber, C.; Ahlrichs, R. *J. Chem. Phys.* **1994**, *100*, 5829–5835.

(45) Kepenekian, M.; Robert, V.; Le Guennic, B. *J. Chem. Phys.* **2009**, *131*, 114702/1–114702/8.

(46) Dey, A.; Ghosh, A. *J. Am. Chem. Soc.* **2002**, *124*, 3206–3207.

(47) Due to the systematic error of the original CASPT2 zero-order Hamiltonian for states with different numbers of unpaired electrons, we did not use the original CASPT2 zero-order Hamiltonian to calculate relative energies of doublet $Fe^V$ states.

(48) Roos, B. O.; Veryazov, V.; Conradie, J.; Taylor, P. R.; Ghosh, A. *J. Phys. Chem. B* **2008**, *112*, 14099–14102.

(49) de Visser, S. P.; Ogliaro, F.; Shaik, S. *Chem.—Eur. J.* **2001**, *7*, 4954–4960.

(50) (a) Neese, F. *Coord. Chem. Rev.* **2009**, *253*, 526–563. (b) Neese, F. *J. Biol. Inorg. Chem.* **2006**, *11*, 702–711.

(51) (a) Neese, F. *J. Chem. Phys.* **2003**, *119*, 9428–9443. (b) Neese, F.; Petrenko, T.; Ganyushin, D.; Olbrich, G. *Coord. Chem. Rev.* **2007**, *251*, 288–327.

(52) (a) Shaik, S.; Danovich, D.; Fiedler, A.; Schröder, D.; Schwarz, H. *Helv. Chem. Acta* **1995**, *78*, 1393–1407. (b) Shaik, S.; Filatov, M.; Schröder, D.; Schwarz, H. *Chem.—Eur. J.* **1998**, *4*, 193–199. (c) Filatov, M.; Harris, N.; Shaik, S. *J. Chem. Soc. Perkin Trans. 2* **1999**, 399–410.

(53) It should be noted that the two main configurations of state **6** can be transformed to the main configuration of state **5** by orbital mixing within the two FeO $\pi^*$ orbitals (resulting in $\pi^*$ orbitals rotation around Fe−O axis). So these two states should be nearly degenerate as long as the two FeO $\pi^*$ orbitals are isotropic around the *xy* plane, as confirmed by the CASPT2/MM results (see Table 2).

(54) (a) Vangberg, T.; Lie, R.; Ghosh, A. *J. Am. Chem. Soc.* **2002**, *124*, 8122–8130. (b) Hirao, H.; Shaik, S.; Kozlowski, P. M. *J. Phys. Chem. A* **2006**, *110*, 6091–6099. (c) Derat, E.; Cohen, S.; Shaik, S.; Altun, A.; Thiel, W. *J. Am. Chem. Soc.* **2005**, *127*, 13611–13621.

(55) (a) Rutter, R.; Hager, L. P. *Biol. Chem.* **1982**, *257*, 7958–7961. (b) Hosten, C. M.; Sullivan, A. M.; Palaniappan, V.; Fitzgerald, M. M.; Terner, J. *J. Biol. Chem.* **1994**, *269*, 13966–13978. (c) Terner, J.; Palaniappan, V.; Gold; Weiss, R.; Fitzgerald, M. M.; Sullivan, A. M.; Hosten, C. M. *J. Inorg. Biochem.* **2006**, *100*, 480–501.

(56) Ghosh, A.; Persson, B. J.; Taylor, P. R. *J. Biol. Inorg. Chem.* **2003**, *8*, 507–511.

(57) Green, M. T. *J. Am. Chem. Soc.* **1999**, *121*, 7939–7940.

(58) Ogliaro, F.; Cohen, S.; Filatov, M.; Harris, N.; Shaik, S. *Angew. Chem., Int. Ed.* **2000**, *39*, 3851–3855.

(59) It should be noted that because the DFT method usually converges to the ground state, and $\sigma_S$ and $a_{2u}$ orbitals are mixed in the gas phase, the $\Sigma_S$ states usually cannot be obtained at this level, but the $^{2,4}\Pi_S$ states could.

(60) For the purpose of comparison with previous gas phase results in ref 14, these values are calculated by using the original CASPT2 zero-order Hamiltonian.

(61) (a) Chen, K.; Que, L. *J. Am. Chem. Soc.* **2001**, *123*, 6327–6337. (b) Chen, K.; Costas, M.; Kim, J.; Tipton, A. K.; Que, L. *J. Am. Chem. Soc.* **2002**, *124*, 3026–3035. (c) Costas, M.; Que, L. *Angew. Chem., Int. Ed.* **2002**, *41*, 2179–2181. (d) Mas-Ballesté, R.; Que, L. *J. Am. Chem. Soc.* **2007**, *129*, 15964–15972. (e) Company, A.; Gómez, L.; Güell, M.; Ribas, X.; Luis, J. M.; Que, L., Jr.; Costas, M. *J. Am. Chem. Soc.* **2007**, *129*, 15766–15767. (f) Company, A.; Feng, Y.; Güell, M.; Ribas, X.; Luis, J. M.; Que, L.; Costas, M. *Chem.—Eur. J.* **2009**, *15*, 3359–3362. (g) Que, L. *Acc. Chem. Res.* **2007**, *40*, 493–500. (h) Costas, M.; Mehn, M. P.; Jensen, M. P.; Que, L. *Chem. Rev* **2004**, *104*, 939–986.

(62) (a) Bassan, A.; Blomberg, M. R. A.; Siegbahn, P. E. M.; Que, L. *J. Am. Chem. Soc.* **2002**, *124*, 11056–11063. (b) Bassan, A.; Blomberg, M. R. A.; Siegbahn, P. E. M.; Que, L. *Angew. Chem., Int. Ed.* **2005**, *44*, 2939–2941. (c) Bassan, A.; Blomberg, M. R. A.; Siegbahn, P. E. M.; Que, L. *Chem.—Eur. J.* **2005**, *11*, 692–705.

(63) Quionero, D.; Morokuma, K.; Musaev, G.; Mas-Ballesté, R.; Que, L. *J. Am. Chem. Soc.* **2005**, *127*, 6548–6549.

(64) de Oliveira, F. T.; Chanda, A.; Banerjee, D.; Shan, X. P.; Mondal, S.; Que, L., Jr.; Bominaar, E. L.; Münck, E.; Collins, T. J. *Science* **2007**, *315*, 835–838.

(65) (a) Nam, W. *Acc. Chem. Res.* **2007**, *40*, 522–531. (b) Yoon, J.; Wilson, S. A.; Jang, Y. K.; Seo, M. S.; Nehru, K.; Hedman, B.; Hodgson, K. O.; Bill, E.; Solomon, E. I.; Nam, W. *Angew. Chem., Int. Ed.* **2009**, *48*, 1257–1260. (c) Bukowski, M. R.; Koehntop, K. D.; Stubna, A.; Bominaar, E. L.; Halfen, J. A.; Münck, E.; Nam, W.; Que, L. *Science* **2005**, *310*, 1000–1002. (d) Lim, M. H.; Rohde, J. U.; Stubna, A.; Bukowski, M. R.; Costas, M.; Ho, R. Y. N.; Münck, E.; Nam, W.; Que, L. *Proc. Natl. Acad. Sci. U.S.A.* **2003**, *100*, 3665–3670.

(66) (a) Collman, J. P.; Chien, A. S.; Eberspacher, T. A.; Brauman, J. I. *J. Am. Chem. Soc.* **2000**, *122*, 11098–11100. (b) Collman, J. P.; Zeng, L.; Decréau, R. A. *Chem. Commun.* **2003**, 2974–2975.

(67) Mekmouche, Y.; Ménage, S.; Toia-Duboc, C.; Fontecave, M.; Galey, J.-P.; Lebrun, C.; Pécaut, J. *Angew. Chem., Int. Ed.* **2001**, *40*, 949–952.

(68) Klopstra, M.; Roelfes, G.; Hage, R.; Kellogg, R. M.; Feringa, B. L. *Eur. J. Inorg. Chem.* **2004**, 846–856.

(69) Nielsen, A.; Larsen, F. B.; Bond, A. D.; Mckenzie, C. J. *Angew. Chem., Int. Ed.* **2006**, *45*, 1602–1606.

(70) Lee, S. H.; Han, J. H.; Kwak, H.; Lee, S. J.; Lee, E. Y.; Kim, H. J.; Lee, J. H.; Bae, C.; Lee, S. N.; Kim, Y.; Kim, C. *Chem.—Eur. J.* **2007**, *13*, 9393–9398.

(71) Lyakin, O. Y.; Bryliakov, K. P.; Britovsek, G. J. P.; Talsi, E. P. *J. Am. Chem. Soc.* **2009**, *131*, 10798–10799.

(72) Kaizer, J.; Klinker, E. J.; Oh, N. Y.; Rohde, J.-U.; Song, W. J.; Stubna, A.; Kim, J.; Münck, E.; Nam, W.; Que, L. *J. Am. Chem. Soc.* **2004**, *126*, 472–473.

(73) (a) Jin, N.; Groves, J. T. *J. Am. Chem. Soc.* **1999**, *121*, 2923–2924. (b) Zhang, R.; Newcomb, M. *J. Am. Chem. Soc.* **2003**, *125*, 12418–12419. (c) Zhang, R.; Horner, J. H.; Newcomb, M. *J. Am. Chem. Soc.* **2005**, *127*, 6573–6582. (d) Song, W. J.; Seo, M. S.; DeBeer George, S.; Ohta, T.; Song, R.; Kang, M.-J.; Tosha, T.; Kitagawa, T.; Solomon, E. I.; Nam, W. *J. Am. Chem. Soc.* **2007**, *129*, 1268–1277.

(74) de Angelis, F.; Jin, N.; Car, R.; Groves, J. T. *Inorg. Chem.* **2006**, *45*, 4268–4276.

(75) (a) Balcells, D.; Raynaud, C.; Crabtree, R. H.; Eisenstein, O. *Chem. Commun.* **2008**, 744–746. (b) Balcells, D.; Raynaud, C.; Crabtree, R. H.; Eisenstein, O. *Inorg. Chem.* **2008**, *47*, 10090–10099. (c) Balcells, D.; Raynaud, C.; Crabtree, R. H.; Eisenstein, O. *Chem. Commun.* **2009**, 1772–1774.

(76) (a) Khenkin, A. M.; Kumar, D.; Shaik, S.; Neumann, R. *J. Am. Chem. Soc.* **2006**, *128*, 15451–15460. (b) Shaik, S.; Hirao, H.; Kumar, D. *Acc. Chem. Res.* **2007**, *40*, 532–542.

(77) (a) Senn, H. M.; Thiel, W. *Angew. Chem., Int. Ed.* **2009**, *48*, 1198–1229. (b) Senn, H. M.; Thiel, W. *Top. Curr. Chem.* **2007**, *268*, 173–290. (c) Senn, H. M.; Thiel, W. *Curr. Opin. Chem. Biol.* **2007**, *11*, 182–187.

(78) (a) Cramer, C. J.; Wloch, M.; Piecuch, P.; Puzzarini, C.; Gagliardi, L. *J. Phys. Chem. A* **2006**, *110*, 1991–2004. (b) Cramer, C. J.; Kinal, A.; Wloch, M.; Piecuch, P.; Gagliardi, L. *J. Phys. Chem. A* **2006**, *110*, 11557–11568. (c) Gherman, B. F.; Heppner, D. E.; Tolman, W. B.; Cramer, C. J. *J. Biol. Inorg. Chem.* **2006**, *11*, 197–205. (d) Cramer, C. J.; Tolman, W. B. *Acc. Chem. Res.* **2007**, *40*, 601–608. (e) Malmqvist, P.-Å.; Pierloot, K.; Shahi, A. R. M.; Cramer, C. J.; Gagliardi, L. *J. Chem. Phys.* **2008**, *128*, 204109/1–204109/10. (f) Gherman, B. F.; Cramer, C. J. *Coord. Chem. Rev.* **2009**, *253*, 723–753. (g) Huber, S. M.; Ertem, M. Z.; Aquilante, F.; Gagliardi, L.; Tolman, W. B.; Cramer, C. J. *Chem.—Eur. J.* **2009**, *15*, 4886–4895. (h) Huber, S. M.; Shahi, A. R. M.; Aquilante, F.; Cramer, C. J.; Gagliardi, L. *J. Chem. Theory Comput.* **2009**, *5*, 2967–2976.

(79) (a) Pierloot, K. *Mol. Phys.* **2003**, *101*, 2083–2094. (b) Pierloot, K.; Vancoillie, S. *J. Chem. Phys.* **2006**, *125*, 124303/1–124303/9. (c) Radoń, M.; Pierloot, K. *J. Phys. Chem. A* **2008**, *112*, 11824–11832. (d) Vancoillie, S.; Pierloot, K. *J. Phys. Chem. A* **2008**, *112*, 4011–4019. (e) Pierloot, K.; Vancoillie, S. *J. Chem. Phys.* **2008**, *128*, 034104/1−124303/11. (f) Vancoillie, S.; Rulisek, L.; Neese, F.; Pierloot, K. *J. Phys. Chem. A* **2009**, *113*, 6149–6157. (g) Radoń, M.; Scebro, M.; Broclawik, E. *J. Chem. Theory Comput.* **2009**, *5*, 1237–1244. (h) Radoń, M.; Broclawik, E.; Pierloot, K. *J. Phys. Chem. B* **2010**, *114*, 1518–1528.

(80) (a) Ghosh, A.; Taylor, P. R. *Curr. Opin. Chem. Biol.* **2003**, *7*, 113–124. (b) Ghosh, A. *J. Biol. Inorg. Chem.* **2006**, *11*, 712–724. (c) Ghosh, A.; Gonzalez, E.; Tangen, E.; Roos, B. O. *J. Phys. Chem. A* **2008**, *112*, 12792–12798. (d) Ghosh, A.; Taylor, P. R. *J. Chem. Theory Comput.* **2005**, *1*, 597–600.

(81) (a) Herebian, D.; Wieghardt, K. E.; Neese, F. *J. Am. Chem. Soc.* **2003**, *125*, 10997–11005. (b) Fouqueau, A.; Mer, S.; Casida, M. E.; Lawson Daku, L. M.; Neese, F. *J. Chem. Phys.* **2004**, *120*, 9473–9486. (c) Fouqueau, A.; Casida, M. E.; Lawson Daku, L. M.; Neese, F. *J. Chem. Phys.* **2005**, *122*, 044110/1−044110/13. (d) Ray, K.; Weyhermüller, T.; Neese, F.; Wieghardt, K. E. *Inorg. Chem.* **2005**, *44*, 5345–5360. (e) Petrenko, T.; Ray, K.; Wieghardt, K. E.; Neese, F. *J. Am. Chem. Soc.* **2006**, *128*, 4422–4436. (f) Sundararajan, M.; Ganyushin, D.; Ye, S. F.; Neese, F. *Dalton Trans.* **2009**, 6021–6036.

(82) (a) Ordejón, B.; de Graaf, C.; Sousa, C. *J. Am. Chem. Soc.* **2008**, *130*, 13961–13968. (b) Kepenekian, M.; Robert, V.; Le Guennic, B.; de Graaf, C. *J. Comput. Chem.* **2009**, *30*, 2327–2333.

(83) Suaud, N.; Bonnet, M.-L.; Boilleau, C.; Labèguerie, P.; Guihéry, N. *J. Am. Chem. Soc.* **2009**, *131*, 715–722.

(84) (a) Jensen, K. P.; Roos, B. O.; Ryde, U. *J. Inorg. Biochem.* **2005**, *99*, 45–54. Erratum: *J. Inorg. Biochem.* **2005**, *99*, 978−978. (b) Ribas-Ariño, J.; Novoa, J. J. *Chem. Commun.* **2007**, 3160–3162.

(85) (a) Gagliardi, L.; Roos, B. O. *Chem. Soc. Rev.* **2007**, *36*, 893–903. (b) Roos, B. O.; Lindh, R.; Cho, H.-G.; Andrews, L. *J. Phys. Chem. A* **2007**, *111*, 6420–6424. (c) Wang, X. F.; Andrews, L.; Lindh, R.; Veryazov, V.; Roos, B. O. *J. Phys. Chem. A* **2008**, *112*, 8030–8037.

(86) Rode, M. F.; Werner, H.-J. *Theo. Chem. Acc.* **2005**, *114*, 309–317.

(87) Paulovič, J.; Cimpoesu, F.; Ferbinteanu, M.; Hirao, K. *J. Am. Chem. Soc.* **2004**, *126*, 3321–3331.

(88) Smith, J. M.; Sadique, A. R.; Cundari, T. R.; Rodgers, K. R.; Lukat-Rodgers, G.; Lachicotte, R. J.; Flaschenriem, C. J.; Vela, J.; Holland, P. *J. Am. Chem. Soc.* **2006**, *128*, 756–769.

(89) (a) Sears, J. S.; Sherrill, C. D. *J. Phys. Chem. A* **2008**, *112*, 3466–3477. (b) Sears, J. S.; Sherrill, C. D. *J. Phys. Chem. A* **2008**, *112*, 6741–6752. (c) Takatani, T.; Sears, J. S.; Sherrill, C. D. *J. Phys. Chem. A* **2009**, *113*, 9231–9236.

(90) (a) Rabilloud, F. *J. Chem. Phys.* **2005**, *122*, 134303/1–134303/6. (b) Polestshuk, P. M.; Sem'yanov, P. I.; Ryabinkin, I. G. *J. Chem. Phys.* **2008**, *129*, 054307/1−054307/13.

(91) Wang, B. W.; Wei, H. Y.; Wang, M. W.; Chen, Z. D. *J. Chem. Phys.* **2005**, *122*, 204310/1–204310/8.

(92) Shearer, J.; Dehestani, A.; Abanda, F. *Inorg. Chem.* **2008**, *47*, 2649–2660.

(93) Chen, H.; Ikeda-Saito, M.; Shaik, S. *J. Am. Chem. Soc.* **2008**, *130*, 14778–14790.

(94) Shaik, S.; de Visser, S. P. In *Cytochrome P450: Structure, Mechanism and Biochemistry*, 3rd ed.; Ortiz de Montellano, P. R., Ed.; Kluwer Academic/Plenum: New York, 2005; pp 45−85.

CT9006234